

Shear Modulus and Specific Heat of the Liquid-Crystal Blue Phases

R. N. Kleiman, D. J. Bishop, R. Pindak, and P. Taborek

AT&T Bell Laboratories, Murray Hill, New Jersey 07974

(Received 13 September 1984)

We report high-precision measurements of the shear modulus, viscosity, and specific heat of cholesteryl nonanoate through its blue phases (BPI–BPIII). For BPI and BPII we find a shear modulus which remains finite as the frequency approaches zero, indicating that they are viscoelastic solids. We find that the cholesteric and BPIII have a viscoelastic behavior similar to each other and that as expected the isotropic phase is a Newtonian fluid. Both our mechanical and calorimetric data show for the first time that BPIII is a stable and distinct thermodynamic phase.

PACS numbers: 64.70.Ew, 61.30.Cz

Many cholesteric liquid crystals exhibit blue phases (BPI–BPIII) over a narrow temperature range (~ 1 K) near the cholesteric \rightarrow isotropic (chol \rightarrow iso) transition. Optical measurements have shown that BPI and BPII have cubic structures,¹ whereas BPIII is composed of helical elements in an unknown arrangement.² We report mechanical and thermodynamic measurements on cholesteryl nonanoate (CN), which exhibits all three blue phases. Previous thermodynamic measurements on CN by Bergmann and Stegemeyer had resolved only two distinct blue phases³ and mechanical measurements on similar compounds were limited to BPI.^{4,5} Both our mechanical and thermodynamic measurements clearly contain features associated with all the transitions in CN (i.e., chol \rightarrow BPI \rightarrow BPII \rightarrow BPIII \rightarrow iso) at temperatures which agree well with the results of optical experiments.¹ Our mechanical measurements stem from an interest in the elastic properties of a three-dimensional structure of defects. Meiboom and co-workers have proposed a model for BPI and BPII which suggests that they are cubic arrays of disclination lines.⁶ The question arises as to whether such phases have a finite shear modulus. We have measured the shear elasticity of the blue phases as a function of frequency at very low shear rates, and confirm that both BPI and BPII exhibit a shear modulus which remains finite as the frequency approaches zero. Furthermore, our mechanical (as well as our heat capacity) results, showing features at the BPII \rightarrow BPIII and BPIII \rightarrow iso transitions, unambiguously establish BPIII as a distinct thermodynamic phase⁷ and shed new light on its nature.

Mechanical measurements were made with use of high- Q (10–25 K) torsional oscillators configured as cup viscometers. The oscillators were driven electrostatically and phase locked at their resonant frequencies of 52, 129, 313, and 1088 Hz. The ampli-

tudes of oscillation were extremely small, to avoid measuring in the plastic flow regime. The resulting maximum shear distortion was $\leq 0.02\%$. The apparatus is described in more detail elsewhere.⁸

The resonant period and amplitude of the oscillator were measured with the cup empty and full. The period shift and amplitude ratio can be converted to a shear elasticity (G) and dynamic viscosity (η). Kestin and Newell and Beckwith and Newell have solved the case of a right cylindrical cup oscillator in contact with a Newtonian liquid (η only).⁹ We have extended this solution to the case of a viscoelastic material (η and G). This solution is *exact* and describes the full crossover regime from damped ($G < \eta\omega$) to underdamped ($G > \eta\omega$) sample motion (the oscillator as a whole is always underdamped), and from viscous penetration depth $\delta \ll$ sample size to $\delta >$ sample size. This calculation is described in detail elsewhere.⁸ We used the values of the density, $\rho(T)$, measured by Price and Wendorff.¹⁰ No calibration constant was required in the conversion to η and G . Here η describes the average energy dissipation under shear, typically ~ 1 P for liquid crystals. η is not the large apparent viscosity (η_{app}), which includes the effects of G in a particular flow geometry.¹¹ All of our samples were polycrystalline, and thus G is the average sample elasticity under shear.

The thermodynamic measurements were made with use of a specially designed adiabatic-type calorimeter operated in a drift mode in which the power required to keep the drift rate dT/dt constant was monitored. This quantity is proportional to the heat capacity of the sample and exhibits peaks at phase boundaries whose size is related to the latent heat of transition.

The CN was obtained from van Schuppen Chemicals and used without further purification. The cup viscometers had a cup radius of 0.51 cm with a sample height from 0.13 to 0.38 cm. The sample size

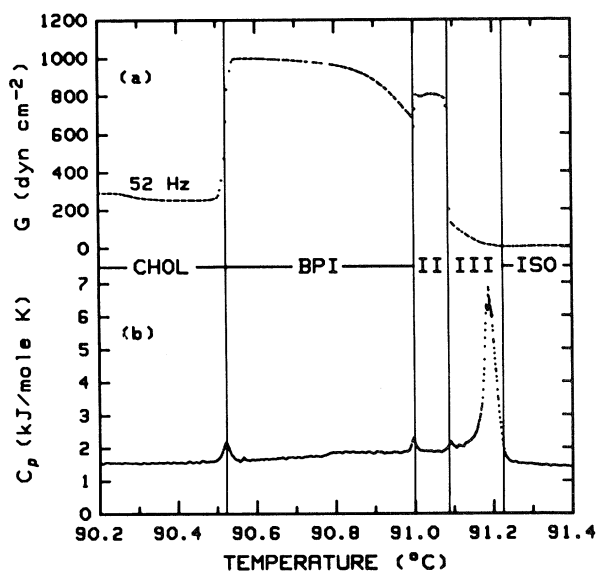


FIG. 1. High-resolution scans of cholesteryl nonanoate, showing the phase boundaries of all three blue phases. (a) Shear elasticity as a function of temperature at 52 Hz. (b) Heat capacity as a function of temperature.

for the calorimeter was 1 g. The first-order transitions supercooled but did not superheat, in particular the BPI → chol transition supercooled as much as 2 K. Thus all data were taken on heating, at extremely slow scan rates: viscometer, 15 mK/h; calorimeter, 60 mK/h. Extreme care was taken to ensure that the temperature stability and gradient across our sample were less than 0.5 mK in all cases.

In Fig. 1(a) a plot of $G(T)$ at 52 Hz is shown. This clearly shows the transitions at the phase boundaries of the three blue phases of CN. Figure 1(b) shows a plot of the heat capacity as a function of temperature, giving a concurring phase diagram, as will be discussed later. We find the following transition temperatures (in degrees Celsius):

$$90.52 \quad 91.00 \quad 91.08 \quad 91.22$$

$$\text{chol} \rightarrow \text{BPI} \rightarrow \text{BPII} \rightarrow \text{BPIII} \rightarrow \text{iso.}$$

With the possible exception of the BPIII → iso transition, all appear to be first order.

Figure 2 shows $G(T)$ and $\eta(T)$ at 129, 313, and 1088 Hz. G increases with increasing frequency in all but the isotropic phase, whereas η decreases with increasing frequency. We see a change in the slope of $G(T)$ and $\eta(T)$ in the middle of BPIII occurring at all frequencies measured, suggesting that the BPIII → iso transition occurs in two steps.

In Fig. 3 we have plotted the frequency dependence of G in the cholesteric and BPI phases. For

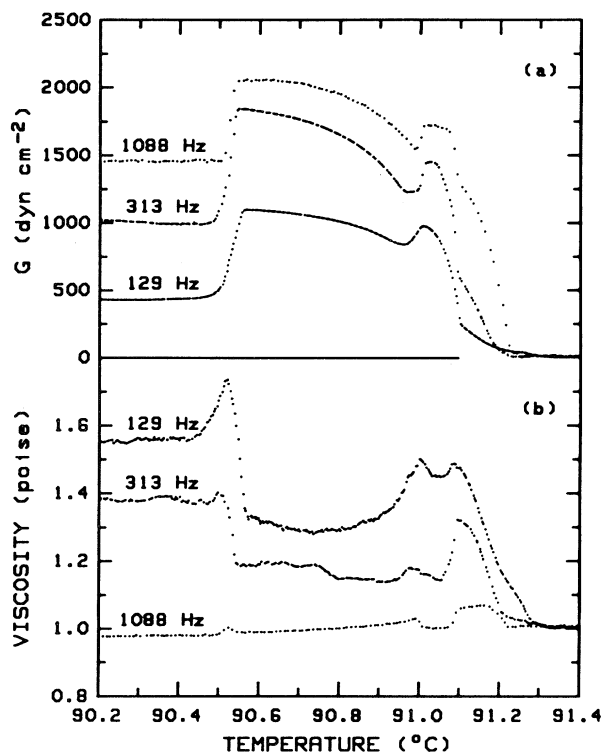


FIG. 2. The shear elasticity (a) and viscosity (b) for CN for different frequencies over the same temperature range as Fig. 1, which includes the cholesteric, BPI, BPII, BPIII, and isotropic phases.

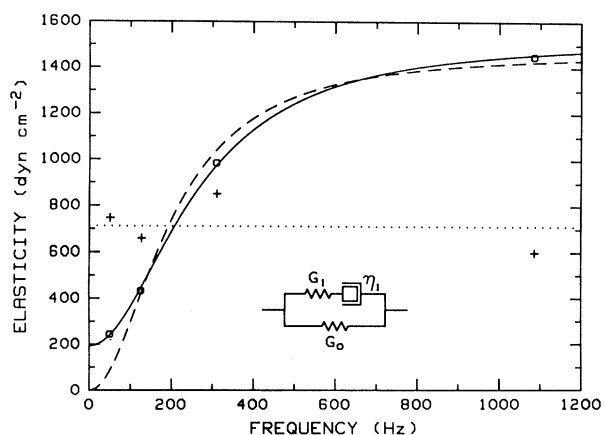


FIG. 3. Shear elasticity of the cholesteric phase (circles) and the increase in elasticity, ΔG , at the chol → BPI transition (pluses) plotted as a function of frequency. G_{chol} goes to a low value, whereas ΔG is finite as ω approaches zero. The solid line corresponds to a best fit using the viscoelastic model shown with $G_1 = 1338 \text{ dyn/cm}^2$, $f_{\text{rel}} = G_1/2\pi\eta_1 = 262 \text{ Hz}$, and $G_0 = 193 \text{ dyn/cm}^2$. The dashed line is a best fit by the same model with G_0 set equal to zero, $G_1 = 1474 \text{ dyn/cm}^2$, and $f_{\text{rel}} = 200 \text{ Hz}$. The dotted line is for $\Delta G = 712 \text{ dyn/cm}^2$.

the cholesteric we plot the value at the chol \rightarrow BPI transition. In the cholesteric phase, G approaches a low value as ω approaches zero. The data can be described mostly simply by the viscoelastic model shown in the inset to Fig. 3, with $G_0 \sim 190$ dyn/cm², $G_1 \sim 1340$ dyn/cm², and a relaxation frequency, $f_{\text{rel}} = G_1/2\pi\eta_1 \sim 260$ Hz. Also shown is a best fit by the same model with G_0 set equal to zero, which clearly worsens the agreement. This indication of a finite value for G_0 is consistent with a low-frequency propagating mode in the cholesteric phase, but further measurements at lower frequencies would be required to confirm this. For BPI we plot the increase in elasticity, ΔG , at the chol \rightarrow BPI transition. ΔG is independent of frequency over the range measured and has a magnitude ~ 710 dyn/cm². This is what we expect for a *viscoelastic solid*.¹² The finite ΔG is due to the topological constraint imposed by the cubic blue-phase lattice, independent of the cholestericlike material composing it. Similar plots for BPII and BPIII show that BPII is similar to BPI, but with $\Delta G \sim 550$ dyn/cm². BPIII is similar to the cholesteric, with G approaching a low value as ω approaches zero. The isotropic phase is what we usually think of as a Newtonian liquid, with $G = 0$ and η constant independent of frequency.

In Fig. 1(b) the heat capacity $C_p(T)$ is shown. All of the features agree in temperature with corresponding features in the mechanical properties, as indicated by the cursors at each phase transition. We find the following latent heats of transition (in joules/mole):

$$\text{chol} \xrightarrow{12.8} \text{BPI} \xrightarrow{6.1} \text{BPII} \xrightarrow{14.0} \text{BPIII} \xrightarrow{193.0} \text{iso.}$$

In BPIII, near the BPII \rightarrow BPIII transition there is a region of constant latent heat absorption. At 91.17°C the absorption of the largest fraction of latent heat in the chol \rightarrow iso transition begins. This occurs at the same temperature as the change in slope in the mechanical properties, confirming the two-step nature of the BPIII \rightarrow iso transition. The width of the final transition is unusually broad, ~ 55 mK, and is not due to instrumental broadening. It may be due to impurity effects, pretransitional effects, or the unusual nature of the phase boundary.

Meiboom and co-workers have proposed a model for the blue phases in which they are composed of a lattice of disclinations with essentially isotropic cores, while the material outside the cores adopts a double twist configuration.⁶ On the basis of optical Bragg scattering and calculations of relative scattering intensities for the observed Bragg peaks, they

have identified BPI as $O^{8(-)}$ (bcc), and BPII as O^2 (sc) in CN.

We can interpret our results for BPI and BPII in the context of this model. If the small change in entropy at the chol \rightarrow BPI transition is assumed to be due to the creation of the isotropic disclination cores, then we can estimate the ratio of the core radius, r , to the blue-phase lattice parameter, d . We find that $r/d \sim 0.051$ for the $O^{8(-)}$ structure. With the measured value of $d = 2164 \text{ \AA}$,¹ this gives $r = 110 \text{ \AA}$. From their model calculations, Meiboom and co-workers find $r/d = 0.024$ for the case $K_{11} = K_{22} = K_{33}$, and $r/d = 0.040$ for the case $K_{11} = 2K_{22} = K_{33}$ for the $O^{8(-)}$ structure⁶ which is consistent with the estimate from our data. The decrease in G through BPI is then due to changes in the disclination core radius, lattice parameter, and elastic constants. The stiffening of G by ~ 275 dyn/cm² at the BPI \rightarrow BPII transition is due to the increase in disclination length per unit volume which accompanies the change in structure. The stiffening may also be attributed to the transition from a structure without intersecting disclination lines ($O^{8(-)}$) to one where they do intersect (O^2). The small change in entropy is associated with the increase in the disclination core volume at the transition.

The mechanical properties of BPIII evolve continuously from being similar to the cholesteric phase at the BPII \rightarrow BPIII transition to being isotropiclike. The large and sharp decrease in G at the BPII \rightarrow BPIII transition is accompanied by only a small change in entropy ($\sim 6\%$). This suggests that, like BPI or BPII, BPIII is composed of disclination lines and double twist cylinders; but that these ordered elements lose the long-range, three-dimensional, positional order which gave them their stiffness. This is consistent with the results for BPIII from optical Bragg scattering of the loss of structure at optical wavelengths but the retention of helicity. We can calculate the degree of disorder of BPIII on the basis of the relative entropy increase, $S(\text{chol} \rightarrow \text{BPIII})/S(\text{chol} \rightarrow \text{iso})$, and find that just above the BPII \rightarrow BPIII transition BPIII still exhibits $\sim 85\%$ cholestericlike order. Nearer to the BPIII \rightarrow iso transition the structure may change to one with a lower surface area, such as an emulsion of double twist elements in the isotropic liquid. It is conceivable for such elements to decrease continuously in size towards the BPIII \rightarrow iso transition, accounting for the width of the BPIII \rightarrow iso transition.

In conclusion, we have mapped out the phase diagram of CN by measuring its mechanical and ther-

modynamic properties as a function of temperature and frequency. BPI and BPII are viscoelastic solids over the frequency range of our measurement. Their behavior can be well understood in the context of the model of Meiboom and co-workers of the blue phases. Both probes show that BPIII is a distinct thermodynamic phase. The question of its structure and the nature of the BPIII \rightarrow iso transition are still open, but it is clear that any model must incorporate the new information presented herein.

The authors would like to acknowledge helpful discussions with S. Meiboom, M. Marcus, and M. Sammon, and thank Gene Benick for the delicate machining of our torsional oscillators, which made the mechanical measurements possible.

¹S. Meiboom and M. Sammon, Phys. Rev. A **24**, 468 (1981).

²M. Marcus, J. Phys. (Paris) **42**, 61 (1981).

³K. Bergmann and H. Stegemeyer, Z. Naturforsch. **34A**, 251 (1979).

⁴N. A. Clark, S. T. Vohra, and M. A. Handschy, Phys. Rev. Lett. **52**, 57 (1984).

⁵P. E. Cladis, P. Pieranski, and M. Joanicot, Phys. Rev. Lett. **52**, 542 (1984).

⁶S. Meiboom, M. Sammon, and W. F. Brinkman, Phys. Rev. A **27**, 438 (1983); S. Meiboom, M. Sammon, and D. W. Berreman, Phys. Rev. A **28**, 3553 (1983).

⁷Supportive evidence for BPIII has recently also been obtained in optical rotatory dispersion measurements by P. J. Collings, Phys. Rev. A **30**, 1990 (1984).

⁸R. N. Kleiman, D. J. Bishop, R. Pindak, and P. Taborrek, to be published.

⁹J. Kestin and G. F. Newell, Z. Angew. Math. Phys. **8**, 433 (1957); D. A. Beckwith and G. F. Newell, Z. Angew. Math. Phys. **8**, 450 (1957).

¹⁰F. P. Price and J. H. Wendorff, J. Phys. Chem. **75**, 276 (1972).

¹¹P. G. de Gennes, *The Physics of Liquid Crystals* (Clarendon, Oxford, 1975), p. 253.

¹²J. D. Ferry, *Viscoelastic Properties of Polymers* (Wiley, New York, 1980), p. 16.